IEEE Access
Multidisciplinary | Rapid Review | Open Access Journal

Received November 13, 2019, accepted January 14, 2020, date of publication February 10, 2020, date of current version February 19, 2020.

Digital Object Identifier 10.1109/ACCESS.2020.2972731

Removing Cardiac Artifacts From Single-Channel Respiratory Electromyograms

EIKE PETERSEN, (Member, IEEE), JULIA SAUER, JAN GRAßHOFF, (Member, IEEE), AND PHILIPP ROSTALSKI, (Member, IEEE)

Institute for Electrical Engineering in Medicine, Universität zu Lübeck, 23562 Lübeck, Germany

Corresponding author: Eike Petersen (eike.petersen@uni-luebeck.de)

This work was supported by the German Federal State Schleswig–Holstein through the Open Access Publikationsfonds Funding Program.

ABSTRACT Electromyographic (EMG) measurements of the respiratory muscles provide a convenient and noninvasive way to assess respiratory muscle function and detect patient activity during assisted mechanical ventilation. However, surface EMG measurements of the diaphragm and intercostal muscles are substantially contaminated by cardiac activity due to the vicinity of the cardiac muscles. Many algorithmic solutions to this problem have been proposed, yet a conclusive performance comparison of the most promising candidates currently is missing. The objective of this work is to provide a quantitative performance comparison of six previously proposed cardiac artifact removal algorithms operating on single-channel EMG measurements, and two newly proposed, improved versions of these algorithms. Algorithmic performance is evaluated quantitatively based on four different measures of separation success, using both synthetic validation signals and electromyographic measurements of the respiratory muscles in eight subjects. The compared algorithms are two versions of the empirical template subtraction algorithm, two model-based Bayesian filtering procedures, a wavelet denoising approach, an empirical mode decomposition (EMD) based approach, and classical high-pass filtering. Different algorithms perform well with respect to different performance measures. Template subtraction algorithms yield the best results if the characteristics of the raw signal are of interest, while filtering algorithms like simple high-pass filtering, wavelet denoising, and EMD-based denoising show superior performance for calculating a cleaned envelope signal. No algorithm completely removes the cardiac interference, but the characteristic errors introduced by the considered algorithms differ. Hence, the choice of the algorithm to use should be made depending on the target application. Finally, we also demonstrate that our empirical SNR measure, which can be calculated without knowledge of the true, undisturbed signals, correlates strongly with the exact reconstruction error. Thus, it represents a reliable indicator for algorithm performance on real measurement data.

INDEX TERMS Adaptive signal processing, biomedical signal processing, electrocardiography, electromyography, electrophysiology, empirical mode decomposition, Kalman filters, signal denoising, source separation, wavelet transforms.

I. INTRODUCTION

Monitoring the activity of the respiratory muscles is of critical importance in respiratory care [1]–[5], and can be achieved continuously and noninvasively using surface electromyography (EMG) [6]–[8]. Unfortunately, the interpretation of EMG measurements of the respiratory muscles is hindered by interference due to cardiac muscle activity. The close vicinity of the recording electrodes to the heart and the strength of the cardiac muscles make cardiac contaminants typically surpass the sought muscle signals by orders of magnitude. Successful removal of cardiac artifacts from the measured signals hence proves crucial for the diagnostic interpretation of respiratory EMG measurements and has engaged researchers for many decades [9], [10]. Note that the estimation of an ECG-derived respiration (EDR) signal is a closely related task that has been considered by many researchers (for a comprehensive review refer to, e.g., Charlton *et al.* [11]). However, EDR estimation is a significantly easier task than recovering the original respiratory EMG signal, as in the EDR scenario, the exact shape of the EMG signal is irrelevant.

In most practical applications, the ECG removal problem is currently solved either by simple high-pass filtering [12], employing QRS gating [13], i.e., by detecting the occurrence

The associate editor coordinating the review of this manuscript and approving it for publication was Emil Jovanov.

of R peaks and then discarding all measurements that are presumably affected by the QRS complex, or using adaptive filtering procedures [14]. The high-pass filtering approach suffers from the fact that the frequency spectra of the ECG and EMG components strongly overlap, rendering the complete removal of ECG interference while maintaining valid EMG signal characteristics impossible. QRS gating mostly guarantees the validity of the remaining signal, but it also requires discarding a significant fraction of the recorded signal and hence cannot be considered an entirely satisfactory solution either. Adaptive filtering algorithms, on the other hand, require the measurement of a reference ECG signal, which is impractical in many applications. Algorithms that allow for the removal of the electrocardiographic (ECG) interference without distorting the original EMG signal and without requiring further measurements are thus highly desirable. Due to the low signal-to-noise ratio (SNR) and overlap in time and frequency domain, this problem is, however, hard to solve. Nevertheless, many authors have proposed solutions to this challenging problem.

The template subtraction (TS) algorithm assumes that the measured signal constitutes an additive mixture of EMG and ECG, with no correlation between the two signals. The algorithm first constructs an ECG beat template as the average of several previously detected consecutive ECG beats and then subtracts this template from each newly detected ECG beat. Such an enhancement of recurring signals through template extraction was first applied in the context of the dual problem, the denoising of ECG signals (see, for instance, Pahlm and Sörnmo [15]). Various versions of template subtraction for the removal of ECG interference from EMG measurements have been suggested [13], [16], [17], and TS is considered the current standard approach.

While the TS algorithm represents a purely empirical method for the removal of ECG interference, Sameni *et al.* [18] proposed a completely different, model-based algorithm based on a dynamical ECG model [19]. In this method, a single ECG beat is modeled as a mixture of Gaussian kernels that represent the different peaks of the ECG signal. A Bayesian filtering procedure (the extended Kalman Filter) is then employed to continuously adjust the model parameters and distinguish between measurement noise and model errors. This approach was further described and refined in subsequent publications [20]–[23].

The wavelet denoising method represents another entirely different approach that has been employed for the solution of a large number of different problems [24], including the removal of ECG interference from EMG measurements [25]–[27]. In this method, the signal is decomposed into several wavelet bands, and a simple threshold is applied in the wavelet domain to detect and remove ECG interference. Sameni *et al.* [21] published the as yet most extensive examination of different wavelets and thresholding strategies concerning the dual problem, the denoising of ECG.

Finally, we have recently proposed the use of the empirical mode decomposition (EMD) method for this problem [28]. The proposed approach is to only compute the first intrinsic mode function (IMF) of the contaminated signal and to use this first IMF as an estimate of the raw EMG signal.

All four algorithmic families – TS, model-based, wavelet-based, and EMD-based algorithms – have been shown to perform well in comparison to other approaches for the removal of cardiac artifacts [21], [25], [28], [29]. In particular, note that single-channel adaptations of the popular adaptive filtering approach [14], on the one hand, have been clearly shown to perform inferior compared to the model-based approaches [21], and on the other hand represent close but less adaptive relatives of the TS algorithm [30].

Previously presented comparisons and validations are based only on numerical simulations [31], a single subject [29], [32], [33], or synthetically generated signals, composed by combining clean EMG measurements with clean ECG measurements [21], [26], [32], [33]. To the author's knowledge, only Slim and Raoof [25] have analyzed real respiratory EMG measurements from multiple subjects, and they only analyzed a single measure of separation success (which is not sufficient, as will be discussed in section V) and only short segments of measurements. No previous study has directly compared the above four families of algorithms to the author's knowledge, although they appear to be the most promising candidates. To conclude, it currently remains unclear which of the algorithms would show superior performance on real measurements obtained from the respiratory muscles.

In this article, we provide a quantitative performance comparison of the template subtraction algorithm, the Bayesian filtering procedure proposed by Sameni *et al.* [21], wavelet denoising, EMD-based denoising, and simple high-pass filtering on single-channel measurements. We focus specifically on strongly interfered EMG measurements with signal-to-noise ratios (far) below 0 dB. To this end, EMG measurements of the respiratory muscles were obtained from eight healthy subjects of varying age, sex, and weight, with each of the measurements lasting about 15 minutes. The performance criteria employed on these real measurement signals are validated using synthetic EMG measurements, obtained from a superposition of non-thoracic EMG measurements and ECG signals. Moreover, we propose a slightly improved version of the template subtraction algorithm and demonstrate its superior performance. We discuss the advantages and disadvantages of each algorithm and attempt to provide a guideline for practical use. Preliminary results of this analysis have been the subject of a workshop publication [28].

II. ALGORITHMS

The following paragraphs briefly present the algorithms under analysis. Figure 1 shows a classification of these fundamentally differing algorithms into frequency filtering methods, peak suppression methods, methods exploiting the quasi-periodicity of the ECG signal, and purely data-driven methods.

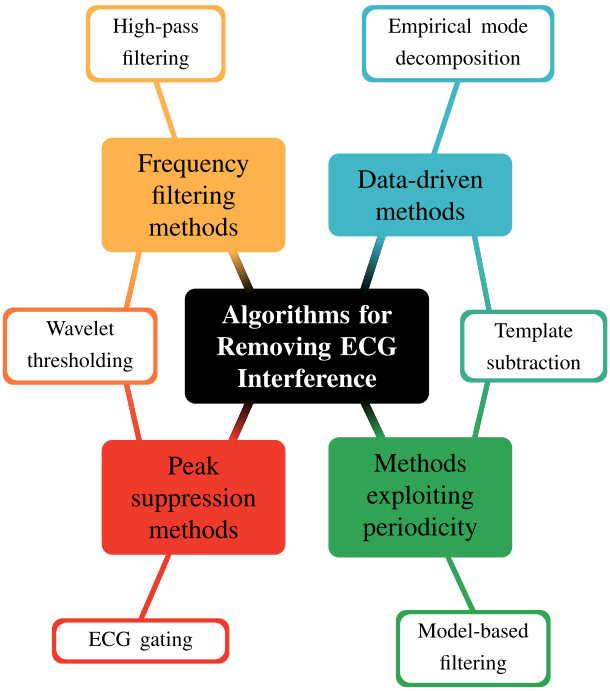

FIGURE 1. Classification of different algorithms for removing ECG interference from single-channel surface EMG measurements.

A. BASIC TEMPLATE SUBTRACTION

The herein used variant of the template subtraction (TS) method can be summarized as follows: First, the locations of the ECG beat peaks in the measurement signal are determined using the algorithm of Pan and Tompkins [34]. For some subjects, due to changing morphologies, different parts of the QRS complex were detected as the maximum peak at different points in time, leading to misaligned beats. For this reason, in a second step, the peak positions are updated by calculating an average beat over the complete data set and re-aligning each detected peak by maximizing correlation with this average beat. The average beat was calculated for this purpose by considering a ± 200 ms window around each detected peak and averaging over all beats. The window size of ± 200 ms was chosen because it contains the most prominent waves (mostly Q, R, S) of a heartbeat, which are relevant for the re-alignment step. The mid-points between two adjacent R peaks determine the boundaries of a single ECG beat; the length of beat i in samples shall be denoted by ℓ_i.

Next, the ECG subtraction template for beat i is constructed by averaging over 40 ECG beats centered around and including the current beat, where for each beat, the samples in a window of length ℓ_i centered around the R peak are considered, similar to the approach of Abbaspour and Fallah [35]. This subtraction template is then aligned with the current ECG beat by maximizing the cross-correlation between the two signals, and the amplitude and offset of the artifact are adjusted by linear regression, i.e., minimizing the squared differences between the current beat and the template. Finally, the resulting template is subtracted from the raw signal, yielding the cleaned EMG measurement. These steps are repeated iteratively for each detected ECG beat.

B. ADAPTIVE TEMPLATE SUBTRACTION

The classical template subtraction method described above usually does not succeed in completely removing the ECG interference from the signal. There are two main reasons for this: Firstly, the amplitude of the ECG interference – particularly during the QRS complex – is so much higher than the amplitude of the EMG signal that even slight deviations of the current beat from the average beat lead to substantial distortions of the cleaned EMG signals. Secondly, the relative positions, amplitudes, and widths of the different ECG peaks vary over time [36], which cannot be compensated for in the classical algorithm since the subtraction template is fit to the current beat as a whole.

To remedy these problems, we propose a slightly improved version of the TS algorithm that still maintains the purely empirical nature of the original algorithm (as opposed to the following, model-based approaches). We propose to modify the original TS algorithm twofold: Firstly, each ECG beat is split into three segments, supposedly representing the P, QRS, and T segments of the beat, and the amplitudes of these three segments are adjusted separately. This segmentation is similar to the adjustments that Akhbari *et al.* et al. [23] made to their original (model-based) algorithm. Secondly, we scale the QRS segment in time in order to fit the QRS complex of the current beat as well as possible, considering that this is the most influential contributor to distortions in the cleaned signal.

In the improved version of the algorithm, which we will call adaptive template subtraction (ATS), we first construct a subtraction template from 40 beats centered around and including the current beat, as described above. We then split this template into three separate segments by assigning a window of 55 ms left and right of the R peak to the middle (QRS) segment of the beat, and the left and right remainders to the other two segments (P and T). Next, differently time-scaled versions of the middle segment of the template are constructed by successively increasing or decreasing the length of the segment towards both sides by up to ± 10 samples, yielding 21 different stretched or shrunk versions of the middle (QRS) segment. To obtain these time-scaled segment versions, we interpolate the original signal values of this segment at the new desired sampling points. A complete subtraction template is then created by concatenating one stretched or shrunk version of the middle segment, and the unmodified left and right template segments, which are cut off or zero-padded to fit the desired beat length ℓ_i. Each of these 21 subtraction templates is aligned separately to the current ECG beat by correlation as in the classical algorithm, and then the three segments of each subtraction template are offset- and gain-adjusted separately by linear regression, as above. Finally, the subtraction template with the lowest sum of squared differences to the current beat is selected and subtracted from the measurement signal to obtain the cleaned EMG measurement.

C. MODEL-BASED FILTERING

A simple yet flexible model for generating synthetic ECG signals has been proposed by McSharry *et al.* [19]. In this model, the ECG waveform is represented by a mixture of Gaussian curves, and the quasi-periodicity of the signal is obtained by orbiting around the unit cycle over time. Each characteristic ECG peak (including but not limited to the standard P, Q, R, S, and T peaks) is modeled to occur in the vicinity of a particular angle of the unit cycle, with one complete orbit corresponding to a whole beat. In the time-discrete polar coordinate formulation of Sameni *et al.* [21], the model reads

$$\theta_{k+1} = f_1(\theta_k, \omega_k) = (\theta_k + \Delta t\, \omega_k) \mod 2\pi \tag{1}$$

$$\begin{aligned} z_{k+1} &= f_2(\theta_k, z_k, \mathbf{a}, \mathbf{b}, \Delta\theta, \omega_k, \eta) \\ &= z_k - \Delta t \sum_{j=1}^{m} \frac{a_j \omega_k}{b_j^2} \Delta\theta_j \exp\left(-\frac{\Delta\theta_j^2}{2b_j^2}\right) + \eta_k, \end{aligned} \tag{2}$$

where z_k denotes the generated ECG signal, θ_k the angle of rotation around the unit cycle, $\Delta\theta_j$ the location of ECG peak j (with $1 \leq j \leq m$) on the unit cycle, Δt the sampling time, ω_k the heart rate and $\mathbf{a} = [a_1 \ldots a_m]^T$ and $\mathbf{b} = [b_1 \ldots b_m]^T$ the (amplitude and width) parameters of the Gaussian waves representing the different ECG peaks. The process noise η_k is assumed to follow a Gaussian distribution.

Sameni *et al.* [21] have proposed the use of the above model for denoising ECG signals and filtering of cardiac contaminants from biomedical signals [22], the latter by subtracting the denoised ECG signal from the measurement signal. To this end, they used an extended Kalman filter (EKF) and extended Kalman smoother (EKS) to estimate the two states θ_k and z_k of the system, while considering all other signals and parameters – $\Delta\theta_j$, ω_k, a_j, b_j and η_k – as Gaussian i.i.d. process noise. The procedure takes two measurement signals, one being the actual measurement, and the second being an artificial phase observation signal that is constructed from the locations of R peaks detected in the signal by the Pan-Tompkins algorithm. They called this filtering method the EKF2/EKS2, with "2" referring to the number of estimated states. Note that while the original publication [21] described the use of just five Gaussian kernels (one for each of the P, Q, R, S, T components of an ECG beat, respectively), later, the number and position of kernels was chosen adaptively [37]. In our implementation, this is performed automatically and up to a number of 13 kernels. For the filtering, we used the implementation provided in the OSET toolbox [37], which employs the innovation signal monitoring proposed by Sameni, Shamsollahi, Jutten, et al. [21] for automatically updating the observation noise covariance online.

Later, Akhbari *et al.* [23] proposed a different Kalman filtering solution using the same dynamical model. Their solution incorporates three separate EKFs for the P, QRS, and T segments of each beat, allowing for different signal dynamics in these three segments. They employ seven Gaussian kernels in total: two for the P and T segments, respectively, and three for the QRS segment. Moreover, they consider all the parameters a_j, b_j and $\Delta\theta_j$ of the Gaussian waves as states of the dynamical system, estimating their values over time as part of the filtering procedure. They call this method the EKF25/EKS25 because the total number of estimated states is 25. To avoid unnecessary matrix inversions, we implemented a sequential version of the extended Kalman filtering procedure [38]. Moreover, we employed the Joseph stabilized version of the covariance measurement update [38] to guarantee that covariance matrices are always symmetric and positive definite. To prevent the b_j estimates from becoming very small, which leads to a very large derivative $\frac{df_2}{db_j}$ and thus filter divergence, we also implemented state constraints using the estimate projection described by Simon [39]. This improvement upon the algorithm described by Akhbari *et al.* [23] leads to a strongly reduced occurrence of outliers on our data set. Finally, for the backward pass, we employed a classical Rauch-Tung-Striebel smoother [38], [40], [41].

D. WAVELET DENOISING

Donoho [42] first suggested the wavelet denoising technique, which is a versatile tool for the denoising of noise and signal mixtures. There is a variety of different denoising strategies, which are characterized by several free design parameters including, for instance, the choice of the decomposition depth, the wavelet family, and the thresholding technique [21]. We found the 4-tap Daubechies wavelet (db2) with three or more levels of decomposition to be a useful choice for ECG-EMG mixtures. As a thresholding strategy, a level-dependent fixed threshold of $4.5\sigma_k$ is used, with σ_k^2 being the estimate for the EMG variance at the k^{th} level of the decomposition.

We suggest three modifications to previous wavelet-based ECG removal approaches [25]–[27]: 1) In contrast to [25] we recommend to use the undecimated, shift-invariant form of the wavelet transform, also called stationary wavelet transform (SWT). The SWT can be interpreted as averaging all possible shifts of the classical wavelet transform and was shown to generally provide higher noise reduction capabilities [43]. 2) As opposed to the dual ECG denoising problem, where usually soft thresholding is applied, we found that the hard thresholding technique gives superior results for the removal of ECG. This is in accordance with the findings of Slim and Raoof [25] and is due to the fact that soft thresholding fails to fully reproduce the amplitude of R peaks. 3) In many wavelet-based denoising applications by default, the median value of decomposition levels is used to estimate the noise variance σ_k^2. We suggest using a moving median filter instead, to compensate for possible changes in the basic EMG noise level within one recording. To further stabilize the noise estimation, the R peaks can be disregarded in the median filter, which minimizes the influence of ECG coefficients on the EMG noise estimation. The described wavelet-based approach yields a denoised version of the ECG component, which is then subtracted from the raw signal to

recover the EMG component. 4) As opposed to Abbaspour and Fallah [26] and Abbaspour *et al.* [27], who used an adaptive filtering method as an additional preprocessing step, we applied our wavelet denoising method to the raw EMG signal.

E. EMPIRICAL MODE DECOMPOSITION

The EMD algorithm [44] constitutes a signal decomposition in the time domain using a purely data-driven approach. Several EMD-based denoising schemes have been proposed in the literature in the context of denoising single-channel physiological measurements, involving adaptive filtering [45], independent component analysis [46], canonical correlation analysis [47] and shrinkage techniques similar to wavelet denoising [48]. For the case of strong ECG interference, we have found empirically [28] that the EMG signal is often entirely contained in the first IMF, while the ECG component is present in higher IMFs. Using this assumption, our ECG removal approach based on the algorithm provided by Rato *et al.* [49] is particularly efficient because the decomposition procedure can be stopped after the calculation of the first IMF and directly yields the denoised EMG [28].

F. HIGH-PASS FILTERING

Following Redfern *et al.* [12], many authors have considered simple high-pass filtering with a cutoff frequency of 30 Hz as an ECG removal algorithm. Empirically, we did not find this to yield acceptable results on our data, likely due to the very low SNR caused by recording close to the heart. In our subsequent performance analysis, we included a fourth-order Butterworth high-pass filter with a cutoff frequency of 200 Hz (HP200), which we found to perform reasonably well, as well as a concatenation of the adaptive TS (ATS) algorithm and the HP200.

Although we did not find high-pass filters with a low cutoff frequency to remove cardiac activity sufficiently well on their own, we *did* find them to significantly simplify the ECG removal task for most other subsequent algorithms, and hence we used them as a preprocessing step in most cases. For most algorithms, we used a 6^{th} order Butterworth filter with a cutoff frequency of 20 Hz. The two Kalman filter-based algorithms are specifically designed to work well for the standard characteristic shape of the ECG signal and hence did not work well for higher cutoff frequencies without significant modifications. For these two algorithms only, we, therefore, used a second-order Butterworth filter with a cutoff frequency of 10 Hz. Finally, we found the wavelet denoising algorithm to perform best when applied to the raw signal, without any additional high-pass filtering. This observation appears to be a result of the algorithm generally working best when dealing with signals of very low SNR.

All linear filters described in this article have been implemented as zero-phase Butterworth high-pass filters in second-order sections form for improved numerical stability.

III. VALIDATION

The fundamental challenge for the validation of cardiac artifact removal algorithms lies in the fact that no ground truth is available: Either an EMG signal is undisturbed by cardiac interference, then there is no problem to be solved, or it is disturbed by it, then there is no way of knowing what the uncontaminated signal would have been. Validation can hence only be indirect and rely on heuristics. To increase the reliability of our analysis, we employ two very different validation methods and draw inferences about algorithm performance taking both their results into account.

First, the algorithms were applied to artificially created, synthetic signals, similar to the approaches of Sameni *et al.* [21], [22], Drake *et al.* [32] and Willigenburg *et al.* [33], among others. These signals are generated by super-posing EMG signals free of cardiac contamination with ECG signals free of EMG contamination. The former is achieved by using EMG signals from a muscle remote from the heart (in our case, the *musculus gastrocnemius*) and performing differential measurements to further minimize cardiac artifacts. For the ECG component, we use standard ECG leads from the PTB diagnostic database [50]. As these are not free of EMG contamination *a priori*, we only used those signals with a noise level below a certain threshold for our validation. For the synthetic signals resulting from the superposition of these two components, the ground truth for ECG removal is known: it is precisely the original, uncontaminated EMG signal. We hence calculated the absolute error attained by each algorithm with respect to the original EMG signal.

Secondly, in order to quantify their performance on real-world signals, the algorithms were applied to real respiratory EMG measurement signals from eight healthy individuals. Separation success was evaluated using two empirical measures: improvement in (estimated) signal-to-noise ratio (SNR) and the amount of ECG-synchronous periodicity remaining in the denoised signal. Note, again, that an exact SNR cannot be calculated in this case, as both the uncontaminated ECG component as well as the uncontaminated EMG component are unknown.

In the following, we describe all steps of the validation procedure in detail.

A. SYNTHETIC TEST SIGNALS

Synthetic ECG-contaminated EMG signals are formed by the superposition of EMG signals measured during contractions of the *musculus gastrocnemius* and ECG signals from the Physionet PTB diagnostic database [50]. Two EMG signals have been measured on a single subject (female, age 21) during both periodic and irregular contractions to enable testing of different scenarios. To simulate differently shaped cardiac artifacts, measurement signals of 15 ECG leads on two healthy subjects have been taken from the Physionet database (Goldberger *et al.* [50], patient ID 131, male, age 26, and patient ID 185, female, age 22). After discarding all ECG signals with a noise level above −30 dB, 22 ECG signals

with noise levels from −47.85 dB to −30.36 dB remained. The noise level was quantified by first pre-filtering the signal by a 20 Hz high-pass filter as discussed above, and then dividing the power of those signal parts outside of a [−70 ms, +450 ms] window around each detected R peak by the power of those parts *within* those windows. The window is the same as used in our empirical SNR estimation, and motivated in section III-D.

All combinations of EMG and ECG signals have been superposed at five different signal-to-noise ratios by scaling the ECG component linearly, i.e.,

$$\mathrm{EMG}_{\mathrm{syn}} = \mathrm{EMG}_{\mathrm{raw}} + k \cdot \mathrm{ECG}_{\mathrm{raw}}. \tag{3}$$

The SNR range of the resulting synthetic measurements (as defined by eq. (8) below), again pre-filtered by a 20 Hz high-pass filter as discussed above, is −42.64 dB to −9.68 dB with a median of −29.44 dB, which is very close to the range of SNRs found in the real measurement signals described in the following section. In total, the above procedure yielded 220 synthetic test signals, each with a duration of 115 seconds. Note that variability in the ECG component was considered the most relevant factor for our analysis as the ECG wave shape mostly determines the success of the removal procedure. We thus used as much as 22 different ECG signals mixed with two characteristic EMG signals for the validation of the algorithms.

B. STUDY DATA

Respiratory EMG measurements were obtained in a trial admitted by the ethics committee of the Universität zu Lübeck (case number 26-165). Four male and four female test subjects aged 21 to 50 (median 22) with no known cardiorespiratory diseases were selected for participation. Care was taken to achieve a high inter-subject variability in physical fitness and body fat percentage; body-mass-index (BMI) range was 17 to 35 with a median of 24.5. For the study, subjects lay in the supine position and breathed through an external inspiratory airway resistance (PowerBreathe Medic, POWERbreathe International Ltd.) to ensure sufficiently strong respiratory muscle activity. Each trial session lasted approximately 15 minutes, with surface EMG measurements of the intercostal muscles and the diaphragm and the airway pressure being recorded simultaneously. Two pairs of pre-gelled, disposable electrodes were placed bilaterally on the costo-abdominal margin and above the second intercostal space with a common ground electrode placed directly above the sternum. EMG signals were measured using the Shimmer3 EMG amplifier (Realtime Technologies Ltd.) with a sampling rate of 1024 Hz, and airway pressure was measured using a differential pressure sensor (MP3V5050, Freescale Semiconductors, Inc.) placed between the inspiratory airway resistance and the mouthpiece. For two subjects, we had to discard one measurement channel due to strong non-cardiac artifacts, leaving 14 EMG measurements in total. All signals were assessed by an expert clinician with respect to cardiac anomalies. None were found, except for (possibly respiration-related) sinus arrythmia in one subject.

For all algorithms except for wavelet denoising, the EMG signals were preprocessed to remove baseline wander and motion artifacts in the low-frequency region, as well as to simplify the following ECG removal task, by applying a high-pass filter with a cutoff frequency of 10 Hz or 20 Hz, as described in detail in section II-F. Power line interference was suppressed using a second-order Butterworth band-stop filter with a stop frequency of 50 Hz. The min-max range of the SNR of the 20 Hz-filtered signals as defined by eq. (8) below across all data sets is −39.94 dB to −6.44 dB, with a median of −28.67 dB. Thus, all signals were strongly disturbed by cardiac artifacts.

C. REMOVAL ERROR

For the synthetic signals, the error introduced by the different ECG removal algorithms in recovering the original, raw EMG signal $\mathrm{EMG}_{\mathrm{raw}}$ can be quantified exactly. We consider the normalized raw error norm

$$e_{\mathrm{raw}} = \frac{\|\mathrm{EMG}_{\mathrm{raw}} - \mathrm{EMG}_{\mathrm{cleaned}}\|_2}{\|\mathrm{EMG}_{\mathrm{raw}}\|_2} \tag{4}$$

of the absolute error signal e between the reference EMG signal $\mathrm{EMG}_{\mathrm{raw}}$ and the denoised signal $\mathrm{EMG}_{\mathrm{cleaned}}$, normalized by the raw EMG signal power. As we are mainly interested in the average performance of the algorithms, extreme outliers are discarded by rejecting samples for which

$$|\mathrm{EMG}_{\mathrm{cleaned}}| > |\max\{\mathrm{ECG}_{\mathrm{raw}}\}| \tag{5}$$

is true. In addition to the errors introduced in recovering the raw EMG activity, we are also interested in the effect that these errors have on an envelope signal calculated using the cleaned EMG signal. As mainly the shape of the envelope is of interest, and not so much the absolute amplitude or the offset, we consider the linear regression

$$\beta_1^*, \beta_0^* = \underset{\beta_1,\beta_2}{\operatorname{argmin}} \|\overline{\mathrm{EMG}}_{\mathrm{raw}} - \beta_1 \overline{\mathrm{EMG}}_{\mathrm{cleaned}} - \beta_0\|_2 \tag{6}$$

to calculate the normalized envelope error norm

$$e_{\mathrm{env}} = \frac{\|\overline{\mathrm{EMG}}_{\mathrm{raw}} - \beta_1^* \overline{\mathrm{EMG}}_{\mathrm{cleaned}} - \beta_0^*\|_2}{\|\overline{\mathrm{EMG}}_{\mathrm{raw}}\|_2} \tag{7}$$

where $\overline{\mathrm{EMG}}$ denotes the centralized mean absolute value (MAV) envelope signal, calculated with a window length of 128 samples.

D. SNR ANALYSIS

The EMG to ECG signal-to-noise ratio (SNR) of measured data can only be assessed heuristically, as the two signals are not separately available. To estimate the SNR empirically, we require a procedure to automatically detect measurement phases with strong EMG activity and low ECG interference, and, conversely, phases with strong ECG interference and low EMG activity. For the calculation of the EMG signal power, sections during inspiration (as detected by automatic

inspection of the airway pressure signal) in between the QRS complexes have been used, similar to the procedure proposed by Bartolo *et al.* [13]. To minimize cardiac activity in the phases used for estimating EMG signal power, values in a window around each detected R peak have been discarded. The window was designed to comprise both the QRS peak as well as the T wave, which were found to contain most of the cardiac signal power. To this end, we chose a window width of 70 ms to the left of the detected R peak and 450 ms to the right of the peak.

For the estimation of the ECG signal power, we performed the inverse of the procedure described above: signals were only considered during expiration (which was assumed to be passive), and only in the [−70 ms, +450 ms] window around each detected R peak. Finally,

$$\mathrm{SNR}\{\mathrm{EMG}_{\mathrm{meas}}\} = 20 \cdot \log_{10} \frac{\mathrm{P}\{H_{\mathrm{BL}}(\mathrm{EMG}_{\mathrm{meas}}(\mathrm{insp} \wedge \neg\mathrm{beat}))\}}{\mathrm{P}\{\mathrm{EMG}_{\mathrm{meas}}(\neg\mathrm{insp} \wedge \mathrm{beat})\}}, \quad (8)$$

where $\mathrm{P}\{X\} = \mathbb{E}\{X^2\}$ denotes the power of signal X, is used to assess the signal (EMG) to noise (ECG) ratio in a given measured or somehow processed signal $\mathrm{EMG}_{\mathrm{meas}}$, in decibels. Here, $H_{\mathrm{BL}}(\cdot)$ denotes a baseline filter which is required to remove any P wave activity from the supposed muscular activity. For this, we used a 6th order zero-phase Butterworth high-pass filter with a cutoff frequency of 25 Hz. To quantify algorithm performance, the SNR improvement

$$\Delta\,\mathrm{SNR}\{\mathrm{EMG}_{\mathrm{cleaned}}\} = \mathrm{SNR}\{\mathrm{EMG}_{\mathrm{cleaned}}\} - \mathrm{SNR}\{\mathrm{EMG}_{20\,\mathrm{Hz}}\} \quad (9)$$

was considered for each data set and each algorithm, where $\mathrm{EMG}_{20\,\mathrm{Hz}}$ denotes the measured EMG signal, preprocessed by the 20 Hz high-pass filter described in section II-F.

For the synthetic signals, both signal components (EMG and ECG) are available individually, and hence, more direct ways of calculating an SNR are available. To achieve consistency of analyses and results between synthetic and real measurement signals, however, we define the SNR in this case using eq. (8) as well. Note that for the synthetic signals, no pressure signal is available. Hence, we selected sections of muscular activity in the EMG signal by applying a fixed threshold: if the absolute of at least one-fifth of the samples contained in a 100-sample window centered around the current sample is greater than 15 mV, the sample is assumed to contain muscular activity.

E. PERIODICITY MEASURE

As a third measure of algorithm performance, we employed the periodicity measure (PM) proposed by Sameni *et al.* [22], which quantifies the amount of signal periodicity synchronous with the cardiac pace. Their measure correlates samples in one ECG beat to samples at a similar phase in the successive beat. For each sample, the time distance τ_k to its sibling sample in the next beat is defined by

$$\tau_k = \min\{\tau \mid \Phi_{k+\tau} = \Phi_k, \tau > 0\}, \quad (10)$$

where Φ_k is a linear phase signal obtained by interpolating from 0 to 2π between two neighboring R peaks. The PM of a signal x is then defined as the Pearson coefficient of correlation [22]

$$\mathrm{PM} = \frac{|\mathbb{E}\{x_k x_{k+\tau_k}\}|}{|\mathbb{E}\{x_k^2\}\,\mathbb{E}\{x_{k+\tau_k}^2\}|^{\frac{1}{2}}}. \quad (11)$$

A signal fully periodic with the heartbeat is indicated by $\mathrm{PM} = 1$; a signal with no periodic component at the heart rate is indicated by $\mathrm{PM} = 0$. Note that while macroscopic measures of respiratory activity *are* correlated with cardiac activity due to, e.g., sinus arrhythmia, this is not to be expected for the raw EMG signal. In analogy to the SNR improvement, we considered the logarithmic PM improvement

$$\Delta\mathrm{PM}\{\mathrm{EMG}_{\mathrm{cleaned}}\} = 20 \cdot \log_{10} \frac{\mathrm{PM}\{\mathrm{EMG}_{20\,\mathrm{Hz}}\}}{\mathrm{PM}\{\mathrm{EMG}_{\mathrm{cleaned}}\}} \quad (12)$$

as an indicator of algorithmic performance for each data set and each algorithm.

IV. RESULTS

A. SYNTHETIC TEST SIGNALS

Figure 2A shows the median of e_{raw} as defined by eq. (4) over all synthetic signals for each removal algorithm, as a function of the SNR of the 20 Hz pre-filtered signal. TS, ATS, and the model-based filtering algorithms perform better for higher SNR than in the low-SNR setting, while all other algorithms show very consistent performance across input SNRs. In general, and especially at relatively high SNRs, the two template subtraction algorithms and the EKS2 yield the best results with respect to the raw EMG signal. All other algorithms attain relative errors close to 1, indicating that their results should not be interpreted as the true, underlying EMG signal.

Results for the envelope error (see fig. 2B) are similar in that the performance of the TS and model-based algorithms depends on the input SNR, while all other algorithms show relatively consistent performance across SNRs. An interesting and significant difference to the raw error results is that the TS algorithms perform significantly *worse* than all the other algorithms except for the EKS25, which performs very poorly in general (we will discuss possible reasons for this in the discussion section). This result is exactly opposite to the behavior observed when considering the raw error. In general, the relative envelope error is also much smaller than the relative raw error. The combination of ATS and HP200 shows the best performance, closely followed by the HP200 alone.

One important limitation of this validation technique results from the presence of measurement noise in the ECG components of the synthetic signals (see section III-A). Since part of this noise has the same characteristics as the added EMG component – it may well *be* EMG activity – any ECG removal algorithm can only recover the sum of the EMG component and the ECG measurement noise. This is not an issue as long as the power of the EMG component is

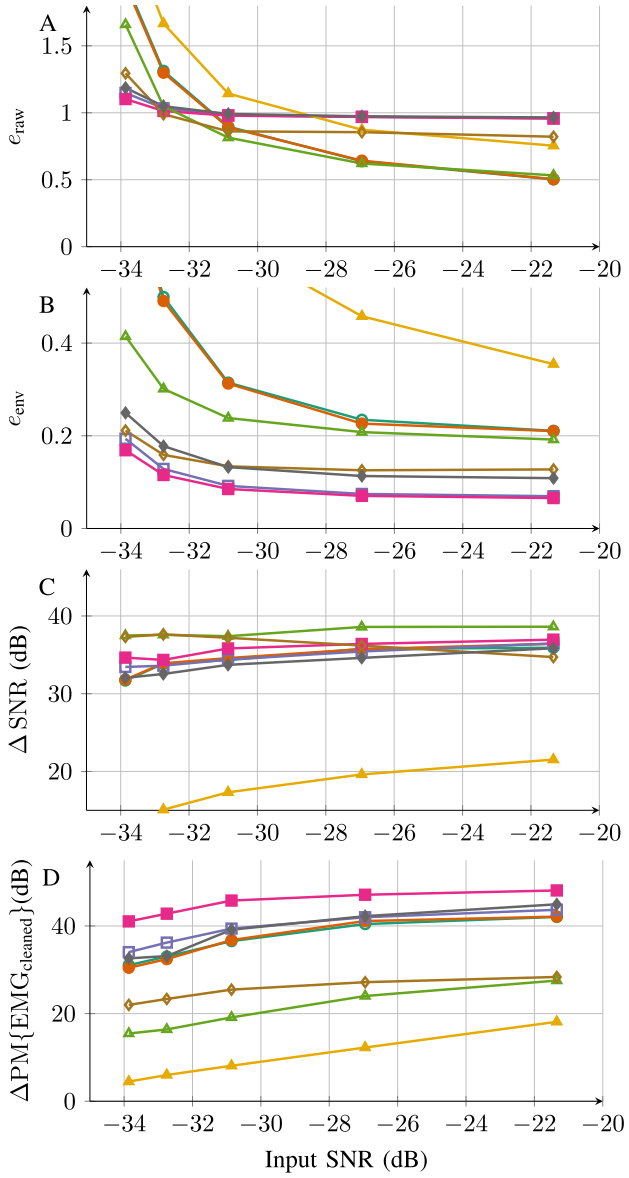

FIGURE 2. (A) Relative pointwise error (see eq. (4)), (B) relative error of the EMG envelope (see eq. (7)), (C) SNR improvement (see eq. (9)) and (D) PM improvement (see eq. (12)) achieved by the different algorithms on synthetic signals. The x axis represents the input SNRs of the synthetic signals as defined by eq. (8), calculated on the 20 Hz pre-filtered signals. The y axis represents the median of the respective performance measure over all 44 synthetic datasets at that particular SNR. The different lines show the results obtained by the TS (○), ATS (●), ATS+HP200 (■), EKS2 (△), EKS25 (▲), HP200 (□), SWT (◇), and EMD (◆) algorithms. The TS curve is hidden by the ATS curve in many regions, because these two algorithms perform very similarly.

significantly greater than the power of the ECG measurement noise. For input SNR values below −30 dB, however, this is no longer the case, and hence both error measures essentially become invalid. This can be observed in fig. 2: For input SNR values below −30 dB, both error measures increase sharply for all algorithms.

We also assessed the utility of the two empirical performance measures introduced in section III-D and section III-E.

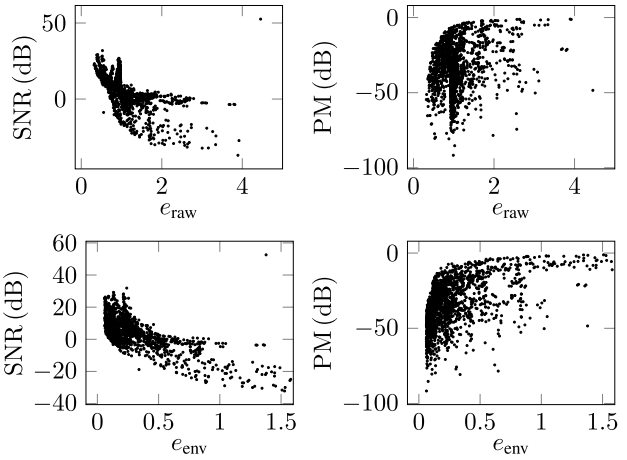

FIGURE 3. Relation of the four discussed performance measures. Each of the 1760 data points in each graph represents one synthetic data set (of which there are 220) processed by one of the eight algorithms under consideration.

Figure 3 depicts the relationship between the two exact performance measures e_{raw} and e_{env}, and the empirical measures SNR and PM in the same subject. A clear, if noisy, correlation can be observed. We calculated Spearman's rank correlation coefficient for all four diagrams. To prevent confounding, we controlled for e_{env} when calculating the correlation of SNR and PM with e_{raw}, and *vice versa*. Considering only those validation signals with input SNR greater than −30 dB – for the reasons discussed above –, the resulting partial correlation coefficients are −0.72 (e_{raw} and SNR), 0.02 (e_{raw} and PM), -0.69 (e_{env} and SNR) and 0.60 (e_{env} and PM). Figure 2C and D show the performance of the examined algorithms in terms of SNR and PM on the synthetic signals.

Finally, we also considered the spectral filtering properties of the different algorithms: Figure 4 shows the power spectral density (PSD) of an exemplary synthetic measurement, the corresponding raw EMG signal, and the same signal cleaned by the different algorithms. The PSD of the signals cleaned by the two template subtraction algorithms is closest to the PSD of the original signal. The EKS2-cleaned signal is also relatively close, while all other algorithms induce significant changes in the spectral content of the signal.

B. STUDY DATA

Figure 5 shows an exemplary subset of the measurements taken from one subject, and the resulting cleaned signals. Figure 6 shows several different envelope signals calculated from the same subset.

Figure 7 (top) shows the calculated SNR improvements achieved by the different algorithms on the measurement signals. All algorithms significantly improve SNR in all recordings, except for the EKS2 which fails completely on one data set. Generally, algorithm performance varies strongly between data sets for all algorithms, with the HP200-algorithms showing the most consistent behavior. Regarding this measure, best median performance is demonstrated by

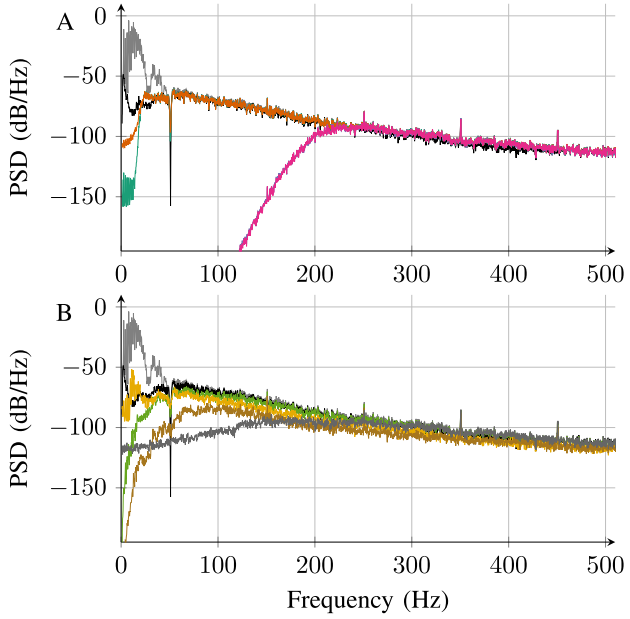

FIGURE 4. Power spectral density (PSD) of an exemplary synthetic measurement (——), the corresponding raw EMG signal (——), and the same signal cleaned by TS (——), ATS (——), HP200 (——), and ATS+HP200 (——) are shown in panel A, and cleaned by EKS2 (——), EKS25 (——), SWT (——), and EMD (——) in panel B. Results are shown for the second-highest of the five SNR levels considered (SNR=−26.95 dB), and PSDs have been computed using Thomson's multitaper method [51].

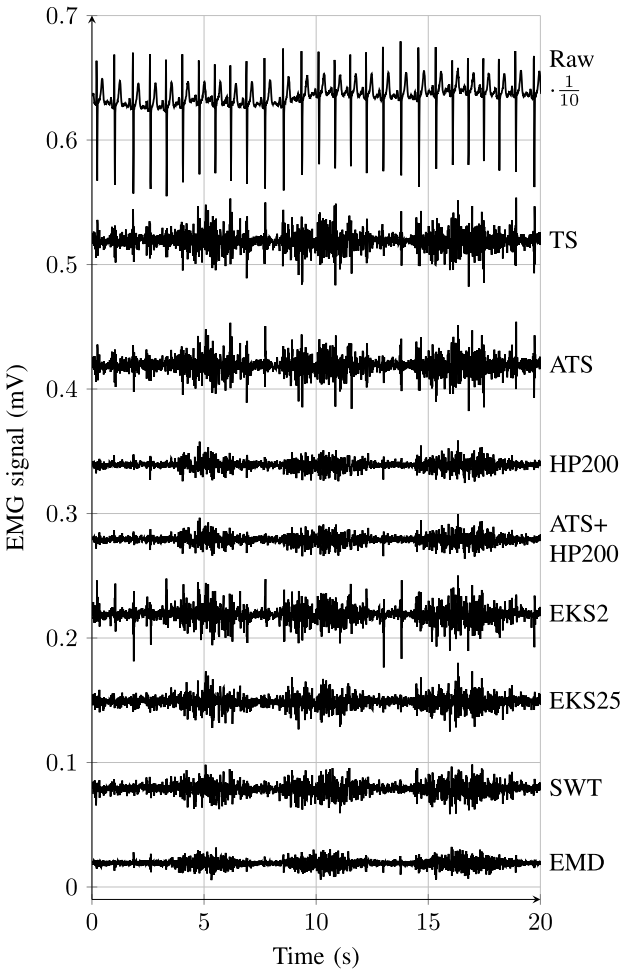

FIGURE 5. Exemplary subset of the measurements taken from subject 7, raw (plotted with a scaling factor of $\frac{1}{10}$) and processed by the various ECG removal algorithms described in the text. All signals are zero-mean, with offsets added for easier comparison.

SWT denoising, closely followed by EKS25 and then the two HP200 algorithms. Note that the EKS25 performance regarding this measure was strongly improved by the introduction of the state projection as described in section II-C (results without state projection not shown here).

Figure 7 (bottom) shows the relative improvements in periodicity measure (PM) achieved by all algorithms. All algorithms reduce the periodicity measure in all recordings; the amount of reduction, however, varies strongly between algorithms and recordings. The periodicity measure is reduced most by the two algorithms involving the HP200, followed by the EMD and the SWT. With the TS and the model-based algorithms, markedly more periodicity remains in the cleaned signal than with the filtering algorithms.

V. DISCUSSION

Evaluating the performance of ECG removal algorithms is a difficult endeavor. Exact performance measures can only be calculated using synthetic data sets, which may, however, not have the same characteristics as real respiratory EMG measurements. Moreover, different performance measures may be of interest, depending on the target application. If, for instance, the exact characteristics of the raw EMG signal are of interest to analyze fatigue measures or muscle onset and offset times [52], other algorithms may be preferable than if a smooth, undisturbed envelope signal is the main target. To address these varying requirements, we considered four different performance measures: the error in reconstructing the raw EMG signal, the error in reconstructing the envelope, the improvement in SNR and the improvement in PM. The first two of these measures were calculated on synthetic signals, the latter two on 14 actual respiratory measurements.

A comparison of these measures on the synthetic signals demonstrates a high degree of correlation (as indicated by Spearman's partial rank correlation coefficient, cf. section IV-A) between both SNR and the two exact error measures e_{env} and e_{raw}, as well as a strong correlation between PM and e_{env}, while PM and e_{raw} are uncorrelated. The latter result is not surprising: PM does not penalize errors in EMG waveform in any way. Hence, while the raw synthetic signal reconstruction error e_{raw} is the only exact measure that quantifies changes to the raw EMG waveform, we have demonstrated that SNR is a reliable indicator as well. Note that considering only one of the two empirical measures in isolation "fails" completely in two extreme cases: The SNR improvement is maximized by performing classical gating (which is not what we desire), and simply setting the whole signal to a constant value will

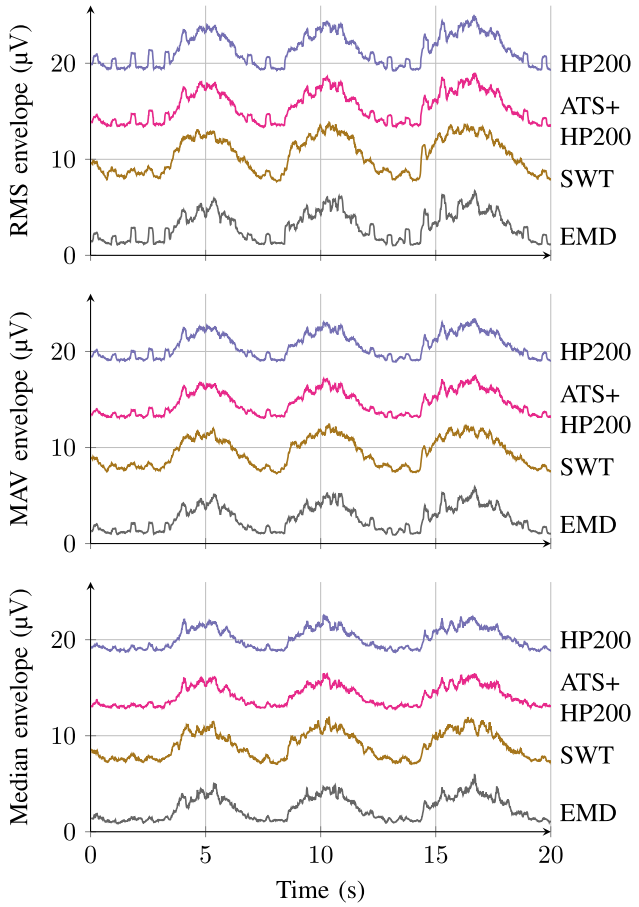

FIGURE 6. Different envelope signals calculated from the signal shown in fig. 5: Root mean square (RMS) envelopes (top), mean absolute value (MAV) envelopes (middle), and median envelopes (bottom). Offsets have been added for easier comparison.

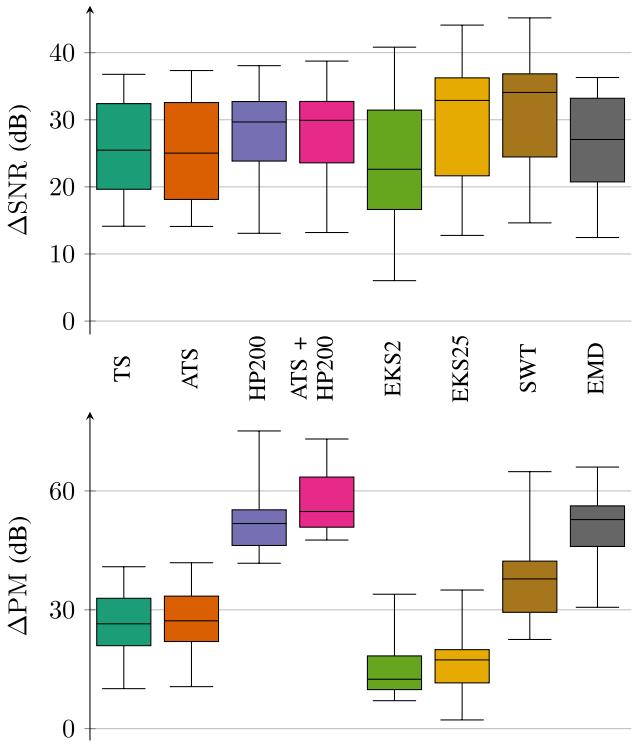

FIGURE 7. Standard box plots (median and inner quartiles; whiskers show the min-max range) for SNR improvement (top) and periodicity measure (PM) improvement (bottom) achieved by all algorithms under consideration, both in dB. In both diagrams, higher values indicate better performance.

yield PM $=$ 1. The two measures complement each other in the sense that if one of them fails, the other still yields a reasonable result. It is worth keeping these limitations in mind while interpreting the results.

Our results generally indicate that for recovering the raw EMG signal without distorting its features, the TS algorithms seem to work best. This result is not very surprising, as these are the only ones of the considered algorithms that perform no filtering of any kind. They cannot introduce any distortion of the EMG signal other than leaving cardiac components present in the signal (unless the true EMG signal is correlated with the heartbeat, which is unexpected for a raw EMG signal). The obvious drawback is that these algorithms typically are unable to remove all cardiac components, leaving enough distortion in the signal to significantly hinder the calculation of envelope signals. As soon as a heartbeat deviates in any way from the average heartbeat, e.g., because of a time-varying heart rate, an artifact remains. Hence, if the raw signal characteristics are of interest, the most suitable solution may be the application of a TS algorithm combined with a residual detection mechanism (which has not been discussed in this article) that detects and removes samples where significant cardiac components remain present. The improved TS algorithm proposed in this paper (ATS) performs slightly better than classical TS on all performance measures with only marginally increased computational effort and hence appears preferable in all cases where a TS algorithm is to be applied.

If, on the other hand, one is mainly interested in the calculation of a clean envelope signal, one of the filtering algorithms (HP200, SWT, EMD) is recommended based on our findings. Based on the results presented here, it is not possible to give a clear recommendation for one of these algorithms as they all perform similarly, and each of them performs best on one of the considered performance measures. It is interesting to note that combining the HP200 with a previous template subtraction procedure improves the results in all cases. In terms of computational efficiency, this is the most efficient solution, followed by the wavelet denoising method, which can be implemented very efficiently using filter banks, and finally, the EMD-based method, which was computationally most demanding. It should also be noted that the computation of a reasonably well-denoised envelope signal does not require highly sophisticated algorithms: using a simple high-pass filter and RMS envelope calculation works quite well (fig. 6, top row). The choice of the envelope calculation method has an impact as well, with the RMS method appearing to yield better results than an MAV envelope, and the median envelope yielding the best results.

The model-based algorithms EKS2 and EKS25 appear to perform poorly in this analysis in comparison to the other algorithms (although EKS25 was already markedly improved by introducing state constraints, as noted above), a result which prompts several remarks. The main problem with these algorithms is, as in most applications of Kalman filter algorithms, the choice of the tuning parameters (the noise covariance matrices): while both algorithms can be tuned to perform exceptionally well on single recordings, we were unable to find rules for the automatic choice of hyperparameters based on data set characteristics that performed equally well on all subjects. Possibly, these algorithms would perform much better if an automatic tuning method was found that efficiently adjusts the noise covariances automatically to each new data set. In parts, this was already implemented in the case of the EKS2, using the automatic adaption of the observation noise covariance based on the innovation process proposed by Sameni *et al.* [21]. However, it is unclear how the remaining parameters – the process noise covariance and the time scale of the observation covariance adaptation – can be automatically and optimally chosen for each new data set. One drawback of the EKS2, as opposed to the EKS25, is that the noise covariance cannot be adapted to the different phases of the ECG beat. For the EKS25, on the other hand, the increased dimension of the noise vectors further aggravates the tuning problem. Aside from this main obstacle of choosing the tuning parameters, some improvements can likely be achieved using better smoothing algorithms: Sameni *et al.* [21] reported slightly improved estimation performance using an unscented Kalman filter (UKF) instead of an EKF, and even better performance could be expected using advanced iterative sigma point filtering and smoothing schemes [53], [54]. We also tested the nonlinear phase observation proposed by Akhbari *et al.* [23] but did not find the results to improve over the linear phase observation (results not shown).

There is another large family of algorithms that we did not consider here, and these are algorithms based on the combination of signal decomposition and source separation techniques, e.g., wavelet-ICA and EMD-ICA [55]–[57]. We do not consider these algorithms here because the selection of the identified components to be suppressed by the algorithm usually requires manual intervention by the user [56], and we wanted to consider fully automatic methods only for this comparison. Still, these algorithms have shown promising results in several studies [33], [56], [58], and automatic component selection methods like the one proposed by Abbaspour *et al.* [57] would be interesting to evaluate on a more extensive data set in the future.

VI. CONCLUSION

Removing cardiac interference from single-channel surface EMG measurements of the respiratory muscles is a challenging task for which many different algorithms have been proposed. In this article, we examined the performance of eight different algorithms from four fundamentally different methodological classes for the automated removal of strong cardiac interference from respiratory EMG measurements. Six of the algorithms have been proposed previously in the literature, and two of them (adaptive template subtraction and wavelet denoising) are optimized versions of previously proposed algorithms. We considered four different performance criteria for evaluating separation success, using both real respiratory measurements from eight subjects and synthetic signals resulting from the superposition of lower limb muscle surface EMG measurements and ECG signals. By comparison of these measures on synthetic signals, we could demonstrate that our empirical SNR measure, which can be calculated without knowledge of the true, undisturbed signals, strongly correlates with the exact signal reconstruction error. It can hence be considered a reliable indicator of algorithm performance on real measurement data.

Our results indicate, in agreement with previous research, that the choice of the algorithm to use should be made depending on the characteristics of the target application. None of the examined algorithms was able to completely suppress the cardiac component from the strongly interfered signals we considered; however, the characteristics of the remaining distortion differ between algorithms. If the raw EMG signal characteristics are of interest, for example, for fatigue analysis [52], algorithms based on the template subtraction method should be preferred because they minimize distortions to the EMG waveform and are simple and easy to implement. If, however, more qualitative features of the EMG signal are of interest, for example, for general quantification of muscular activity through envelope calculation, filtering algorithms are preferable. In particular, we found the wavelet denoising method, our EMD-based filtering method, and simple high-pass filtering (possibly enhanced by previous application of template subtraction) to perform best for this purpose. We also evaluated two model-based filtering methods, which showed great potential considering individual data sets but proved difficult to adjust to different data sets automatically, currently limiting their fully automated application.

CODE AVAILABILITY

The implementation of all algorithms used during the preparation of this article and data from two of our study subjects are available on the Code Ocean platform for computational reproducibility: https://doi.org/10.24433/CO.0394646.v1. There, the complete data analysis including all necessary steps can also be executed online.

ACKNOWLEDGMENTS

The authors would like to thank N. Carbon, Department of Anesthesiology, and Operative Intensive Care Medicine, Charité Universitätsmedizin Berlin, Germany, for assessing our study data with respect to cardiac anomalies. Furthermore, they would also like to thank the anonymous reviewers, whose valuable comments helped to greatly improve this article.

REFERENCES

[1] A. H. Jonkman, D. Jansen, and L. M. A. Heunks, "Novel insights in ICU-acquired respiratory muscle dysfunction: Implications for clinical care," *Crit. Care*, vol. 21, no. 64, Mar. 2017.
[2] C. Sinderby, S. Liu, D. Colombo, G. Camarotta, A. S. Slutsky, P. Navalesi, and J. Beck, "An automated and standardized neural index to quantify patient-ventilator interaction," *Crit. CareCrit Care*, vol. 17, no. 5, p. R239, 2013.
[3] E. C. Goligher, E. Fan, M. S. Herridge, A. Murray, S. Vorona, D. Brace, N. Rittayamai, A. Lanys, G. Tomlinson, J. M. Singh, S.-S. Bolz, G. D. Rubenfeld, B. P. Kavanagh, L. J. Brochard, and N. D. Ferguson, "Evolution of diaphragm thickness during mechanical ventilation. Impact of inspiratory effort," *Amer. J. Respiratory Crit. Care Med.*, vol. 192, no. 9, pp. 1080–1088, Nov. 2015.
[4] T. Yoshida, V. Torsani, S. Gomes, R. R. De Santis, M. A. Beraldo, E. L. V. Costa, M. R. Tucci, W. A. Zin, B. P. Kavanagh, and M. B. P. Amato, "Spontaneous effort causes occult Pendelluft during mechanical ventilation," *Amer. J. Respiratory Crit. Care Med.*, vol. 188, no. 12, pp. 1420–1427, Dec. 2013.
[5] T. Mauri *et al.*, "Esophageal and transpulmonary pressure in the clinical setting: Meaning, usefulness and perspectives," *Intensive Care Med.*, vol. 42, no. 9, pp. 1360–1373, Sep. 2016.
[6] E. J. W. Maarsingh, L. A. Van Eykern, A. B. Sprikkelman, M. O. Hoekstra, and W. M. C. Van Aalderen, "Respiratory muscle activity measured with a noninvasive EMG technique: Technical aspects and reproducibility," *J. Appl. Physiol.*, vol. 88, no. 6, pp. 1955–1961, Jun. 2000.
[7] M. L. Duiverman, Leo A. van Eykern, P. W. Vennik, G. H. Koëter, E. J. W. Maarsingh, and P. J. Wijkstra, "Reproducibility and responsiveness of a noninvasive EMG technique of the respiratory muscles in COPD patients and in healthy subjects," *J. Appl. Physiol.*, vol. 96, no. 5, pp. 1723–1729, May 2004.
[8] A. A. Koopman, R. G. T. Blokpoel, L. A. van Eykern, F. H. C. de Jongh, J. G. M. Burgerhof, and M. C. J. Kneyber, "Transcutaneous electromyographic respiratory muscle recordings to quantify patient–hventilator interaction in mechanically ventilated children," *Ann. Intensive Care*, vol. 8, no. 1, p. 12, Jan. 2018.
[9] R. V. Lourenco and E. P. Mueller, "Quantification of electrical activity in the human diaphragm," *J. Appl. Physiol.*, vol. 22, no. 3, pp. 598–600, Mar. 1967.
[10] E. P. Mueller and R. V. Lourenco, "On-line subtraction of the cardiac activity from the esophageal electromyogram of the diaphragm," *IEEE Trans. Biomed. Eng.*, vol. BME-15, no. 2, pp. 115–118, Apr. 1968.
[11] P. H. Charlton, T. Bonnici, L. Tarassenko, D. A. Clifton, R. Beale, and P. J. Watkinson, "An assessment of algorithms to estimate respiratory rate from the electrocardiogram and photoplethysmogram," *Physiol. Meas.*, vol. 37, no. 4, pp. 610–626, Apr. 2016.
[12] M. Redfern, R. Hughes, and D. Chaffin, "High-pass filtering to remove electrocardiographic interference from torso EMG recordings," *Clin. Biomech*, vol. 8, no. 1, pp. 44–48, Jan. 1993.
[13] A. Bartolo, C. Roberts, R. R. Dzwonczyk, and E. Goldman, "Analysis of diaphragm EMG signals: Comparison of gating vs. Subtraction for removal of ECG contamination," *J. Appl. Physiol.*, vol. 80, no. 6, pp. 1898–1902, Jun. 1996.
[14] G. Lu, J.-S. Brittain, P. Holland, J. Yianni, A. L. Green, J. F. Stein, T. Z. Aziz, and S. Wang, "Removing ECG noise from surface EMG signals using adaptive filtering," *Neurosci. Lett.*, vol. 462, no. 1, pp. 14–19, Sep. 2009.
[15] O. Pahlm and L. Sörnmo, "Data processing of exercise ECG's," *IEEE Trans. Biomed. Eng.*, vol. 34, no. 2, pp. 158–165, Feb. 1987.
[16] R. Bloch, "Subtraction of electrocardiographic signal from respiratory electromyogram," *J. Appl. Physiol.*, vol. 55, no. 2, pp. 619–623, Aug. 1983.
[17] S. Levine, J. Gillen, P. Weiser, M. Gillen, and E. Kwatny, "Description and validation of an ECG removal procedure for EMGdi power spectrum analysis," *J. Appl. Physiol.*, vol. 60, no. 3, pp. 1073–1081, Mar. 1986.
[18] R. Sameni, M. B. Shamsollahi, C. Jutten, and M. Babaie-Zadeh, "Filtering noisy ECG signals using the extended Kalman filter based on a dynamic ECG model," *Comput. Cardiol.*, vol. 32, pp. 1017–1020, Oct. 2005.
[19] P. Mcsharry, G. Clifford, L. Tarassenko, and L. Smith, "A dynamical model for generating synthetic electrocardiogram signals," *IEEE Trans. Biomed. Eng.*, vol. 50, no. 3, pp. 289–294, Mar. 2003.
[20] R. Sameni, M. B. Shamsollahi, and C. Jutten, "Multi-channel electrocardiogram denoising using a Bayesian filtering framework," in *Proc. Comput. Cardiol.*, Sep. 2006, pp. 185–188.
[21] R. Sameni, M. Shamsollahi, C. Jutten, and G. Clifford, "A nonlinear Bayesian filtering framework for ECG denoising," *IEEE Trans. Biomed. Eng.*, vol. 54, no. 12, pp. 2172–2185, Dec. 2007.
[22] R. Sameni, M. B. Shamsollahi, and C. Jutten, "Model-based Bayesian filtering of cardiac contaminants from biomedical recordings," *Physiol. Meas.*, vol. 29, no. 5, pp. 595–613, May 2008.
[23] M. Akhbari, M. B. Shamsollahi, C. Jutten, A. A. Armoundas, and O. Sayadi, "ECG denoising and fiducial point extraction using an extended Kalman filtering framework with linear and nonlinear phase observations," *Physiol. Meas.*, vol. 37, no. 2, pp. 203–226, Feb. 2016.
[24] S. Mallat, *A Wavelet Tour of Signal Processing: The Sparse Way*. San Diego, CA, USA: Academic, 2008.
[25] Y. Slim and K. Raoof, "Removal of ECG interference from surface respiratory electromyography," *IRBM*, vol. 31, no. 4, pp. 209–220, Sep. 2010.
[26] S. Abbaspour and A. Fallah, "A combination method for electrocardiogram rejection from surface electromyogram," *Open Biomed. Eng. J.*, vol. 8, no. 1, pp. 13–19, Mar. 2014.
[27] S. Abbaspour, A. Fallah, M. Lindén, and H. Gholamhosseini, "A novel approach for removing ECG interferences from surface EMG signals using a combined ANFIS and wavelet," *J. Electromyography Kinesiol.*, vol. 26, pp. 52–59, Feb. 2016.
[28] J. Grasshoff, E. Petersen, and P. Rostalski, "Removing strong ECG interference from EMG measurements," in *Proc. Workshop BIOSIG*, Erfurt, Germany, Mar. 2018, pp. 47–48.
[29] P. Zhou and T. A. Kuiken, "Eliminating cardiac contamination from myoelectric control signals developed by targeted muscle reinnervation," *Physiol. Meas.*, vol. 27, pp. 1311–1327, Oct. 2006.
[30] J. Graßhoff, E. Petersen, M. Eger, G. Bellani, and P. Rostalski, "A template subtraction method for the removal of cardiogenic oscillations on esophageal pressure signals," in *Proc. Ann. Int. IEEE EMBS*, Jul. 2017, pp. 2235–2238.
[31] Y. Deng, W. Wolf, R. Schnell, and U. Appel, "New aspects to event-synchronous cancellation of ECG interference: An application of the method in diaphragmatic EMG signals," *IEEE Trans. Biomed. Eng.*, vol. 47, no. 9, pp. 1177–1184, Sep. 2000.
[32] J. D. Drake and J. P. Callaghan, "Elimination of electrocardiogram contamination from electromyogram signals: An evaluation of currently used removal techniques," *J. Electromyography Kinesiol.*, vol. 16, no. 2, pp. 175–187, Apr. 2006.
[33] N. W. Willigenburg, A. Daffertshofer, I. Kingma, and J. H. van Dieën, "Removing ECG contamination from EMG recordings: A comparison of ICA-based and other filtering procedures," *J. Electromyography Kinesiol.*, Jun. 2012.
[34] J. Pan and W. J. Tompkins, "A real-time QRS detection algorithm," *IEEE Trans. Biomed. Eng.*, vol. 32, no. 3, pp. 230–236, Mar. 1985.
[35] S. Abbaspour and A. Fallah, "Removing ECG artifact from the surface EMG signal using adaptive subtraction technique," *J. Biomed. Phys. Eng.*, vol. 4, no. 1, pp. 33–38, Mar. 2014.
[36] M. L. Simoons and P. G. Hugenholtz, "Gradual changes of ECG waveform during and after exercise in normal subjects," *Circulation*, vol. 52, pp. 570–577, Oct. 1975.
[37] R. Sameni. (2006). *Open Source ECG Toolbox*. [Online]. Available: https://www.oset.ir
[38] D. Simon, *Optimal State Estimation*. Hoboken, NJ, USA: Wiley, 2006.
[39] D. Simon, "Kalman filtering with state constraints: A survey of linear and nonlinear algorithms," *IET Control Theory Appl.*, vol. 4, no. 8, pp. 1303–1318, Aug. 2010.
[40] H. E. Rauch, F. Tung, and C. T. Striebel, "Maximum likelihood estimates of linear dynamic systems," *AIAA J.*, vol. 3, no. 8, pp. 1445–1450, Aug. 1965.
[41] S. Särkkä, *Bayesian Filtering Smoothing*. Cambridge, U.K.: Cambridge Univ. Press, 2013.
[42] D. L. Donoho, "De-noising by soft-thresholding," *IEEE Trans. Inf. Theory*, vol. 41, no. 3, pp. 613–627, May 1995.
[43] M. Lang, H. Guo, J. E. Odegard, C. S. Burrus, and R. O. Wells, "Noise reduction using an undecimated discrete wavelet transform," *IEEE Signal Process. Lett.*, vol. 3, no. 1, pp. 10–12, Jan. 1996.
[44] N. E. Huang, Z. Shen, S. R. Long, M. C. Wu, H. H. Shih, Q. Zheng, N.-C. Yen, C. C. Tung, and H. H. Liu, "The empirical mode decomposition and the Hilbert spectrum for nonlinear and non-stationary time series analysis," *Proc. Roy. Soc. A, Math. Phys.*, vol. 454, no. 1971, pp. 903–995, Mar. 1998.

[45] M. Rakshit and S. Das, "An efficient ECG denoising methodology using empirical mode decomposition and adaptive switching mean filter," *Biomed. Signal Process. Control*, vol. 40, pp. 140–148, Feb. 2018.
[46] B. Mijović, M. De Vos, I. Gligorijević, J. Taelman, and S. Van Huffel, "Source separation from single-channel recordings by combining empirical-mode decomposition and independent component analysis," *IEEE Trans. Biomed. Eng.*, vol. 57, no. 9, pp. 2188–2196, Sep. 2010.
[47] K. T. Sweeney, S. F. McLoone, and T. E. Ward, "The use of ensemble empirical mode decomposition with canonical correlation analysis as a novel artifact removal technique," *IEEE Trans. Biomed. Eng.*, vol. 60, no. 1, pp. 97–105, Jan. 2013.
[48] A. O. Andrade, S. Nasuto, P. Kyberd, C. M. Sweeney-Reed, and F. Van Kanijn, "EMG signal filtering based on empirical mode decomposition," *Biomed. Signal Process. Control*, vol. 1, no. 1, pp. 44–55, Jan. 2006.
[49] R. Rato, M. Ortigueira, and A. Batista, "On the HHT, its problems, and some solutions," *Mech. Syst. Sig. Process.*, vol. 22, no. 6, pp. 1374–1394, Aug. 2008.
[50] A. L. Goldberger, L. A. Amaral, L. Glass, J. M. Hausdorff, P. C. Ivanov, R. G. Mark, J. E. Mietus, G. B. Moody, C.-K. Peng, and H. E. Stanley, "PhysioBank, PhysioToolkit, and PhysioNet," *Circulation*, vol. 101, no. 23, pp. e215–e220, Jun. 2000.
[51] D. B. Percival and A. T. Walden, *Spectral Analysis for Physical Applications*. Cambridge, U.K.: Cambridge Univ. Press, 1993.
[52] E. A. Clancy, D. Farina, and G. Filligoi, "Single-channel techniques for information extraction from the surface EMG signal," in *Electromyography: Physiology, Engineering, and Noninvasive Applications*, R. Merletti and P. A. Parker, Eds. Hoboken, NJ, USA: Wiley, 2004.
[53] F. Tronarp, A. F. Garcia-Fernandez, and S. Sarkka, "Iterative filtering and smoothing in nonlinear and non-Gaussian systems using conditional moments," *IEEE Signal Process. Lett.*, vol. 25, no. 3, pp. 408–412, Mar. 2018.
[54] C. Herzog, E. Petersen, and P. Rostalski, "Iterative approximate nonlinear inference via Gaussian message passing on factor graphs," *IEEE Control Syst. Lett.*, vol. 3, no. 4, pp. 978–983, May 2019.
[55] V. von Tscharner, B. Eskofier, and P. Federolf, "Removal of the electrocardiogram signal from surface EMG recordings using non-linearly scaled wavelets," *J. Electromyography Kinesiol.*, vol. 21, no. 4, pp. 683–688, Aug. 2011.
[56] K. T. Sweeney, T. E. Ward, and S. F. McLoone, "Artifact removal in physiological signals–practices and possibilities," *IEEE Trans. Inf. Technol. Biomed.*, vol. 16, no. 3, pp. 488–500, May 2012.
[57] S. Abbaspour, M. Lindén, and H. Gholamhosseini, "ECG artifact removal from surface EMG signal using an automated method based on wavelet-ICA," in *Proc. pHealth*, 2015, pp. 91–97.
[58] E. Petersen, H. Buchner, M. Eger, and P. Rostalski, "Convolutive blind source separation of surface EMG measurements of the respiratory muscles," *Biomed. Eng.*, vol. 62, no. 2, pp. 171–181, Apr. 2017.

EIKE PETERSEN (Member, IEEE) received the B.Sc. degree in computer science and engineering from the Hamburg University of Technology, Germany, in 2012, and the M.Sc. degree in industrial mathematics from Hamburg University, Germany, in 2015, having spent one semester at the Institut National des Sciences Appliquées, Toulouse, France. He is currently pursuing the Ph.D. degree with the Institute for Electrical Engineering in Medicine, Universität zu Lübeck, Germany.

During the entire term of his studies, he was with Dräger Medical GmbH, Lübeck, Germany, working on various scientific problems related to signal processing and mechanical ventilation. Since 2015, he has been working as a Research Associate with the Institute for Electrical Engineering in Medicine, Universität zu Lübeck. His most current projects are related to surface electromyography (EMG), respiration, or both. His research interests are at the intersection of mathematical modeling, signal processing, parameter identification, and statistical inference, all driven by several biomedical applications.

JULIA SAUER received the B.Sc. and M.Sc. degrees in medical engineering science from Universität zu Lübeck, Germany, in 2016 and 2019, respectively, where she is currently pursuing the Ph.D. degree with the Institute for Electrical Engineering in Medicine.

From 2016 to 2017, she was a Research Assistant with the Institute for Electrical Engineering in Medicine, Universität zu Lübeck. From 2017 to 2018, she did an Internship with the Development Team at VisiConsult, Stockelsdorf, Germany.

JAN GRAßHOFF (Member, IEEE) received the B.Sc. and M.Sc. degrees in computer science from Universität zu Lübeck, Germany, in 2014 and 2016, respectively, where he is currently pursuing the Ph.D. degree with the Institute for Electrical Engineering.

For the master's degree thesis, he was with the Research Unit, Dräger Medical, Germany, where he was working on respiratory parameter and state estimation. Since 2016, he has been working as a Research Associate with the Institute for Electrical Engineering, Universität zu Lübeck. His research interests include probabilistic signal processing and parameter/state estimation problems in biomedical applications. In particular, he works on respiratory signal processing and system modeling in the context of mechanical ventilation.

PHILIPP ROSTALSKI (Member, IEEE) received the Dipl.Ing. degree in electrical engineering with a focus on measurement and control from the Hamburg University of Technology, Germany, in 2004, and the Ph.D. degree, in 2009.

In 2005, he joined the Automatic Control Laboratory with ETH Zürich, Switzerland, where he worked at the interface of algebraic geometry, optimization, and control. After several international research exchanges, he completed the Ph.D. degree, in 2009. He joined the Department of Mathematics with UC Berkeley, in 2009, and the Department of Mechanical Engineering as a Feodor Lynen Fellow of the German Alexander von Humboldt Foundation later in 2010 where he was working on problems in applied mathematics, most notably on convex algebraic geometry. From 2011 and 2015, he was a Research Engineer and the Project Manager of mechatronics applications with the Dräger Research Unit, Lübeck, Germany. He was responsible for projects in signal processing and control, with a focus on pneumatic systems and respiratory care. Since 2015, he has been the Director of the Institute for Electrical Engineering in Medicine, Universität zu Lübeck, Germany.

Prof. Rostalski's Ph.D. thesis was awarded with the ETH Medal for outstanding Ph.D. theses.